19th IFAC Symposium on Automatic Control in Aerospace
September 2-6, 2013. Würzburg, Germany

Spacecraft with Very High Pointing Stability: Experiences and Lessons Learned

Norimasa Yoshida*, Osamu Takahara, Kazuhide Kodeki*****

**Advanced Technology R&D Centre, Mitsubishi Electric Corp., Amagasaki, Hyogo, 661-8661 Japan (Tel: 06-6497-7161; e-mail: Yoshida.Norimasa@bx.MitsubishiElectric.co.jp).*
***Kamakura Works, Mitsubishi Electric Corp., Kamakura, Kanagawa, 247-8520 Japan (e-mail:Takahara.Osamu@ds.MitsubishiElectric.co.jp)*
****Advanced Technology R&D Centre, Mitsubishi Electric Corp., Amagasaki, Hyogo, 661-8661 Japan (e-mail: Kodeki.Kazuhide@db.MitsubishiElectric.co.jp)*

Abstract: Technical issues associated with spacecraft with very high pointing stability requirement for short to medium term (typically, sub-micro radians for 1-100 seconds) are reviewed. Specifically, microvibration and pointing jitter, that are induced by various internal disturbance sources, is a major issue for this class of satellite. The experiences and lessons learned through the development of several satellites are presented. In particular, some basic concepts on attitude and pointing, new evaluation techniques of pointing stability, influence of high frequency microvibration on pointing and attitude, and dynamic interface between payload and bus are described in this context.

Keywords: Attitude control, Disturbance, Pointing systems, Space vehicle optical-controls-structure interaction (O-CSI), Vibration Measurement

1. INTRODUCTION

There is a class of spacecraft, especially in the field of astronomy, earth observation and meteorology, that requires very tight pointing stability or relative pointing error (RPE). For example, the solar observations satellite SOLAR-B("Hinode", see Figure 1), that carries three mission instruments, the Solar Optical Telescope (SOT), the X-Ray Telescope (XRT) and the Extreme Ultra-Violet Imaging Spectrometer (EIS) and was launched in 2006, requires the short-term pointing stability of 0.06 arcsec (roughly equal to 0.3 μrad) (3σ) for the time duration of 10 seconds for the SOT, and 0.6-1.1 arcsec (roughly equal to 3-5 μrad) (3σ) over 1-20 seconds for XRT/EIS [Yoshida (2004 & 2012), Kosugi (2005)]. Other examples are Hubble Space Telescope that requires pointing stability of 0.007 arcsec (rms) or 0.021 arcsec (3σ) for 10s -24hrs [Dougherty (1982), Griffin (1984) and Jedrich (2002)], and Herschel that requires RPE of 0.3 arcsec for 1 min [Schmidt (2012)]. For earth observations satellite in low earth orbit (LEO) such as IKONOS, GeoEye, WorldView and Pleiades, the short-term RPE requirement is thought to be in the order of 0.05 arcsec or 0.2 μrad (3σ) for 1 ms, assuming the satellite altitude ~500-800 km, GSD ~0.5m, TDI ~20 stages, and the LOS stability requirement during exposure time ~0.1*GSD(1σ).

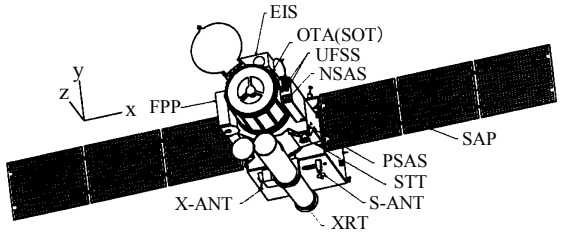

Fig. 1. In-orbit configuration of SOLAR-B ("Hinode") [Takahara (2005)]

For this class of spacecraft with very high pointing stability requirement (typically sub-micro radians over 1-1000 seconds for astronomical mission and over 0.1-1 ms for LEO earth observations mission), several technical issues emerge as crucial that would not have been critical at all for spacecraft with lower requirement. Such technical issues are discussed, and experiences and lessons learned through the development of several satellites such as SOLAR-B (Hinode) are presented. In particular, some basic concepts on attitude and pointing, new evaluation techniques of pointing stability, influence of microvibration on pointing and attitude, and dynamic interface between payload and bus are described in this context.

2. MAJOR TECHNICAL ISSUES

2.1 Internal Disturbance and Microvibration

Numerous internal disturbance sources exist within the spacecraft. Representative disturbance sources are reaction/ momentum wheels and control momentum gyros for attitude control, mechanical gyros for attitude determination, solar paddles and antenna drive mechanisms, cryogenic coolers, various moving mechanisms inside mission payload such as scanning mirrors, phase modulation mechanisms, filter

wheels, focus adjusting mechanisms, etc.. The internal disturbance sources generally induce both disturbance forces and disturbance torques.

The internal disturbances may be classified as is shown in Figure 2. If the frequency component of the steady-state disturbance exists mainly in the low frequency region, either the whole spacecraft or the main body except flexible appendages responds to the disturbance torque about the centre of mass (CM) of the body. But if the frequency spectrum spreads over the higher frequencies, the disturbance forces/torques transmitted via spacecraft and mission payload structure, excite vibration of various parts of the spacecraft. While the disturbance level is very small, the induced vibration level is expected to be small in general, too, e.g., sub-micrometers in displacement or micro-G's in acceleration. Therefore, it is often referred to as "microvibration" [Bétermier (1993), Laurens (1996), Marchante (1997), Jedrich (2002), and Yoshida (2004)].

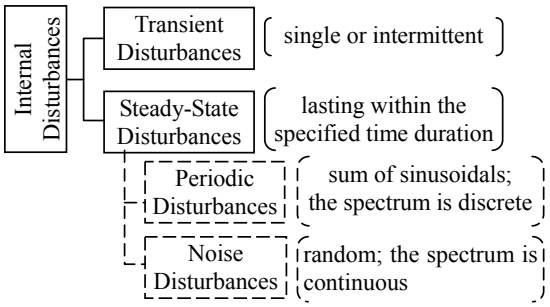

Fig. 2. Classification of internal disturbances [Yoshida (2013)]

However, even if the disturbance and the resultant response level is very small, the induced pointing error may well exceed the specification.

For example, the pointing error induced by a low frequency sinusoidal disturbance is simply evaluated by the following formula, based on the elementary rigid-body dynamics,

$$\Delta\theta = T_D / (I \cdot \omega_D{}^2)$$

where $\Delta\theta$ is the pointing error, T_D is the disturbance torque about the CM of the main body, ω_D is the disturbance frequency, I is the moment of inertia of the main body. It is also assumed here that the main body of the spacecraft except flexible appendages is rigid, the disturbance frequency is beyond the attitude control system (ACS) bandwidth and there is no other device to control pointing of the payload. And the cross-coupling effect through the product of inertia is neglected here. A numerical example is T_D=10^-5 N*m (0-p), ω_D=0.05Hz(~0.3 rad/s) and I=1000 kg*m^2. Then the resultant pointing error will be $\Delta\theta$ ~0.1 μrad(0-p) or 0.2 (=(3/$\sqrt{2}$)*0.1) μrad (3σ). This is unacceptable if the pointing stability requirement is 0.1 μrad (3σ) for 10s. As is seen from this simple example, very small disturbance in low frequency region, that is well below the ordinary measurement limit, might be a big issue for this class of spacecraft.

Another example is high frequency disturbance. In higher frequency region, where the structure of both spacecraft bus and mission payload is no more rigid, the microvibration affects pointing stability of mission payload in different ways. If the disturbance frequency is in the vicinity of the resonant frequency of the sensor block inside the payload, then the block will vibrate inside the payload and an unacceptable level of pointing error may be excited. In still higher frequency region where the sensor block is no more rigid, the optical elements such as the primary mirror and the secondary mirror inside the sensor will move independently. This kind of movements of optical elements cause the line of sight (LOS) jitter of the sensor. The resonant modes in other parts of the spacecraft may also increase the vibration of optical elements. For example, resonance of supporting structure of disturbance sources will amplify the disturbance, and will be transmitted to the optical elements. Thus in high frequency region, there usually exist numerous frequencies of disturbance that will induce high level of pointing jitter.

As the internal disturbance becomes a central issue for this class of spacecraft, how to manage and control internal disturbance within the acceptable level is essential in order to achieve the required performance. Specifically, in the high frequency region, the final performance depends on both disturbance sources and their transfer paths to the pointing error, so that the disturbance control must cover both factors in this region (Figure 3). In the low frequency region, the issue is that the required level of disturbance be often unrealistically small, if the disturbance frequency were beyond the ACS bandwidth. In this case, the sole solution would be the introduction of a pointing control system (PCS) with control bandwidth much wider than that of ACS.

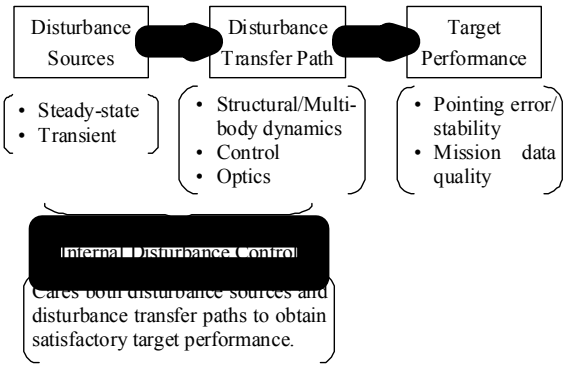

Fig. 3. Internal disturbance control [Yoshida (2013)]

2.2 Estimation, Evaluation and Validation of Performance

Estimation, evaluation and validation of the performance are indispensable for the success of program. As the pointing requirement becomes more stringent, however, the tasks become more difficult, since the level of both disturbance forces/ torques and pointing error that has to be measured, becomes extremely small. Moreover, in high frequency region where many local resonant modes are excited, the disturbance transfer functions are very much complicated, and is almost impossible to predict based on the finite element model (FEM) analysis. This is because any elaborate FEM can hardly simulate the real structural property with sufficient fidelity in high frequency region. Therefore the

measurement is the only reliable way to evaluate the pointing performance before launch.

However, there exist multiple difficulties associated with the measurement. At first glance, the measurement may seem to be feasible with flight model (FM) of the spacecraft "Let's measure the pointing jitter optically by injecting laser beam into the mission payload from outside with actual disturbance sources operated one by one." But, actually, this approach has several problems; (1)The microvibration of the light source may spoil the measurement severely and its rejection may not be easy. (2)How to simulate the free-free boundary condition in orbit is another challenge. (3)Even if the measurement worked, what could we do if the predicted performance were unacceptable. The last one is almost fatal to the program. Consequently, how to estimate or predict the performance as early as possible with sufficient accuracy by measurement, is a crucial issue.

3. EXPERIENCES AND LESSONS LEARNED

3.1 System Design on Frequency-Domain Consideration

In the previous chapter, it was explained that the internal disturbance is a central issue for the class of spacecraft under consideration. It was also mentioned that the system responds quite differently to the disturbances in different frequency region. Therefore, a frequency-domain consideration is of foremost importance in the system design, which will be explained in more detail in this section.

First of all, three frequency regions are defined as follows.

(a) Low frequency region (typ. from DC to 0.01-0.1 Hz) : The region where the whole spacecraft behaves as a rigid body. Almost equal to the ACS bandwidth.

(b) Mid-frequency region (typ. from 0.01-0.1 to 10 Hz) : The region where some appendages with low natural frequencies are flexible, but the central body of bus and payload remains rigid. Usually out of ACS bandwidth, but roughly equal to PCS bandwidth (if any).

(c) High frequency region (typ. over 10 Hz, practically up to 100-1000 Hz) : The region where the whole spacecraft is no more rigid. Well beyond ACS bandwidth and usually out of PCS bandwidth (if any), too.

Conventionally in the ACS design, spacecraft is usually modelled as a central body plus flexible appendages or a central body plus articulated multi-bodies. Either model assumes a rigid central body whose attitude is to be controlled. In these models, however, there exist only the two frequency regions practically: the low frequency region and the high frequency region, where the latter is actually the mid frequency region according to the above classification. In real high frequency region, there is no clear central body, so it is hard to define "attitude" of spacecraft. If the attitude must be defined up to that region for some reasons, one reasonable candidate might be the LOS direction of certain attitude sensor that provides attitude reference for the ACS (e.g., star sensor). And this direction is thought to be equal to the rotation of a hypothetical base plane of the sensor, as long as the sensor is rigid inside. But this attitude represents only that of one specific local point of the structure anyway .

It is also important to recognize that the attitude defined above is completely different from the pointing error in the high frequency region; and there is no correlation between them. In fact, as large as 4 order or more difference exists, as is explained later. Therefore, very precise attitude control, for example, does not guarantee a fine pointing at all.

Another important aspect is the interpretation of the pointing stability requirement in the frequency domain. Figure 4 is an example of the interpretation[Yoshida (2004)]. It corresponds to a set of pointing stability specifications with $\Delta\theta < \Delta\theta_1$ for T_{S1} and $\Delta\theta < \Delta\theta_2$ for T_{S2}. In order to illustrate the importance of the interpretation in the frequency domain, let us consider two pointing stability specifications whose magnitudes are both 0.1 μrad (0-p) but the specified time durations are 1ms and 10s. These are typical numbers for earth observations and astronomical missions, respectively. Then a single frequency sinusoidal pointing error that is equal to the required limit, would be 0.1 μrad (0-p) at 320 Hz(=1/(π*1ms)) or above for both cases. But at 3.2 Hz and 0.032 Hz(=1/(π*10s)), for example, the amplitude limit of the first specification is 2 and 4 order looser than the second one, respectively. Thus it is obvious that the criticality to microvibration is quite different for the two specifications.

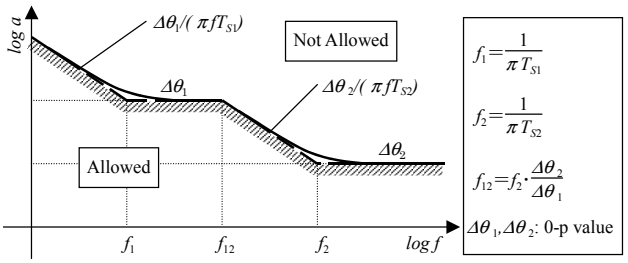

Fig. 4. Frequency domain interpretation of pointing stability [Yoshida (2004)]

3.2 Evaluation and Validation of Performance before Launch

In order to estimate or predict the pointing performance as early as possible, a novel method was invented by the authors and applied to the SOLAR-B (Hinode) project. The method, designated as "disturbance transmissibility test", measures disturbance transfer functions, using a small shaker as an excitation source and the Structural and Thermal Model (STM) of the satellite that includes EM of the mission payload as an object to be measured. Another essential invention associated with the method was the measurement of the pointing jitter using accelerometer arrays, referred to "inertial measurement method", as is illustrated in Figure 5. [Yoshida (2004& 2012), Takahara (2004, 2007 & 2008)].

The disturbance transmissibility test has made it possible to predict the pointing performance at the EM phase, since it does not need any FM components; The disturbance generating components are replaced by their dummy masses, and the disturbance forces/ torques are applied by a shaker.

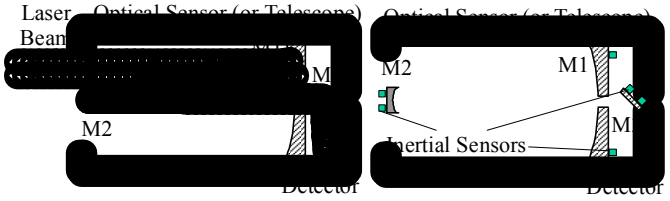

(a) Optical measurement (b) Inertial measurement

Fig. 5. Measurement methods of pointing error

The satellite bus and the mission payload used in the test must be equivalent to FM in terms of mechanical properties. However, it is not necessary for the mission payload to have actual optical components such as polished mirrors and detectors, since the accelerometers are used to estimate pointing jitter. In order to simulate the free-free boundary condition of satellite in orbit, the whole satellite is hanged from the ceiling by long and very soft springs. This configuration also isolates the satellite from the vibration of the building and the floor. Torques as well as forces must be applied, because they excite different resonant modes. And the applied forces/torques must be as small as the actual ones, since the damping factor of structure, that determines peak amplitude of the transfer function, depends on the vibration level. Therefore, a small inertial type (i.e., proof-mass type) shaker was used that could generate the same small level of disturbance as actual, and also to maintain the free-free boundary condition. And a sine excitation with fixed frequency was used in order to simulate the steady-state periodic disturbance. Other reasons why sine excitation, instead of random excitation, is used, are: (1)At least a few tens of periods are necessary to fully develop a resonance in the vicinity of resonant frequencies, that is also expected to occur in orbit at certain conditions (e.g., certain wheel speeds), (2)Since the measured vibration is very small, it is imperative to improve S/N by post processing of data such as narrow band-pass filter and least square fitting, even with the use of accelerometers with high sensitivity, and (3)From a set of data with different excitation points, a pure force or torque input data can be compiled by post-processing.

The quantities to be determined through this measurement are the transfer function matrices $\boldsymbol{G}_i$ from the forces/torques of each disturbance source i to the pointing error $\boldsymbol{\theta}=[\theta_x, \theta_y]^{\mathrm{T}}$.

$$\begin{bmatrix}\theta_x(s)\\ \theta_y(s)\end{bmatrix}=\begin{bmatrix}G_{i,11}(s) & \cdots & G_{i,16}(s)\\ G_{i,21}(s) & \cdots & G_{i,26}(s)\end{bmatrix}\cdot\begin{bmatrix}\boldsymbol{F}_{D,i}(s)\\ \boldsymbol{T}_{D,i}(s)\end{bmatrix}$$

To this end, the transfer functions from each disturbance forces/torques to the translation and rotation (or shift and tilt) of main optical elements are measured first. Then the result is combined with the sensitivity matrices from the shift/tilt of optical elements to the pointing errors. Finally, the pointing performance is predicted by combining the obtained transfer functions with the estimated disturbance forces/torques that are usually provided by the disturbance source manufacturers based on measurement or analysis.

Figure 6 and Figure 7 are examples of the measured transfer functions in Hinode. Figure 6 is the transmissibility from a disturbance force to a shift of the Secondary Mirror(M2), and Figure 7 is the transfer function from another disturbance force to the pointing error about Y axis. Note that the actual vibration level induced by the applied force 0.2 N is only 10-100 nm up to 200 Hz even on the resonant peaks in Figure 6. In this level of microvibration, Q factor was in the order of 100. This indicates the damping factor ζ is about 0.5% in this range. Larger ζ's were observed for larger input forces.

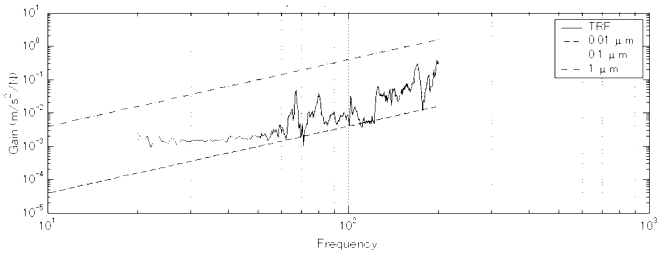

Fig. 6. Typical transmissibility of vibration（F=0.2N, IRU-E to SOT secondary mirror , Z axis）[Yoshida (2004)]

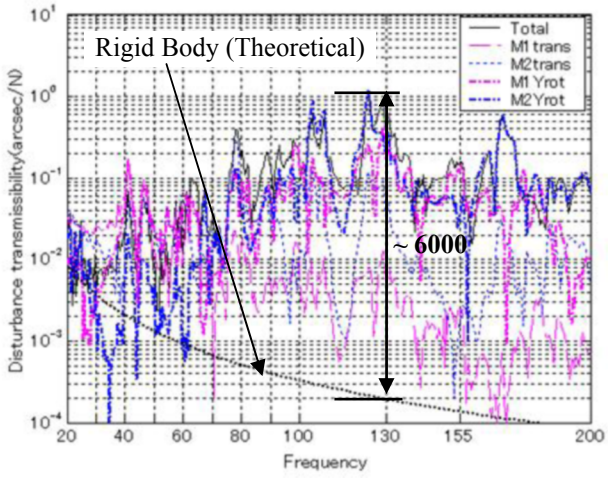

Fig. 7. Measured transmissibility from disturbance force F_X of IRU-B1 to pointing error $\Delta\theta_Y$ (Hinode）[Takahara (2004)]

The transfer function to the pointing error (Figure 7) is much more complicated than that to one point on certain optical element (Figure 6). It is because the transfer function to the pointing error consists of multiple elements with different resonant modes. And due to the optical sensitivities of those elements, the transfer function exhibits amplification of 6000 compared to the ideal rigid body response. Another result shows the amplification factor of 7000 [Yoshida (2004)]. These amplifications can really occur, for example, if some of the disturbance frequencies happen to exist in the vicinity. Specifically, the reaction wheels generate disturbance with many frequency components, and most of them change their frequencies as the wheel speed gradually change in orbit. Therefore there is great possibility that one of the disturbance components approaches to some of the transfer function peak frequencies some time. This was actually observed in Hinode. And the behavior perfectly coincides with the prediction based on the ground test, where an actual wheel was used instead of a shaker and the wheel speed was slowly swept over a wide range.

From Figure 7, it can be said that the pointing error is completely different (as large as 4 order) from the attitude of ideal rigid body in the high frequency region. If the attitude were defined with LOS direction of certain attitude reference sensor, the difference might be much larger, since the LOS direction is thought to be roughly equal to the rotation of the sensor base plate that is also subject to vibration. And the attitude thus defined may be out of phase with pointing jitter.

Subsequent to the "disturbance transmissibility test", the final validation of the pointing performance was performed in Hinode, using FM. The disturbance sources were now actual disturbing components, and the optical measurement method (Figure 5(a)) was adopted. The test was named as the "disturbance response test". The result fairly coincides with the prediction based on the disturbance transmissibility test, but several frequency components were found to be spoiled. This was attributed to the microvibration of the laser light source affected by the environment (floor, test stand, etc.).

In Hinode, the flight data was also analyzed. The Solar Optical Telescope (SOT) of Hinode is furnished with the Pointing Control System called CTM (Correlation Tracker and Tip-Tilt Mirror, see Figure 8). The main roles of CTM are: (1)to suppress the attitude response to very small, low to mid frequency disturbances (if any), (2)to reject attitude control residuals, and (3)to suppress pointing error to many transient disturbances. The control reference sensor CT (Correlation Tracker) detects pointing error by tracking the solar surface pattern, and output the error at about 580 Hz. The output errors transmitted to the ground at the same frequency were used for the evaluation. The evaluated performance during the initial in-orbit test was $\Delta\theta x$=0.0094 arcsec (1σ) and $\Delta\theta y$=0.0075 arcsec (1σ), which was well within the requirement of 0.06 arcsec (3σ) or 0.02 arcsec (1σ) for the time duration of 10 seconds.

Using the same CT data, spectral analysis was performed up to 200Hz. It enabled precise evaluation of the pointing error caused by specific error sources. Figure 9 is an example of the result compared with that the ground test result. The disturbance frequencies are 113Hz (IRU-A) and 155Hz(IRU-B), respectively. The coincidence was fairly good, and was actually much better than expected, considering the big amplification factors as is shown in Figure 7. The result demonstrates the validity of a series of methods to evaluate

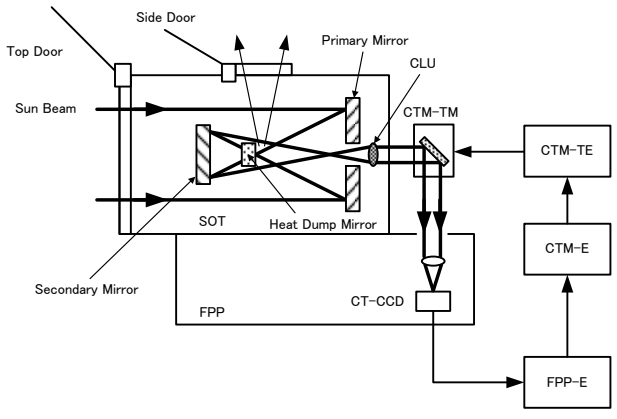

Fig. 8. Functional block diagram of CTM [Kodeki (2007)]

pointing performance before launce. The methods have been successfully applied to many satellites after Hinode at MELCO (Mitsubishi Electric Corp.).

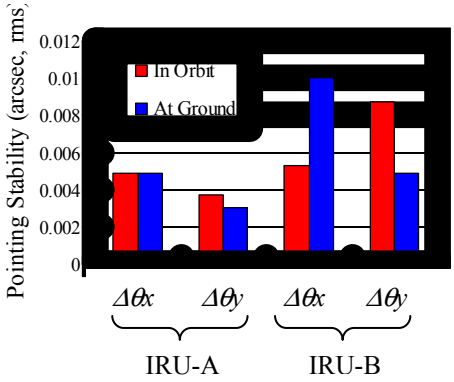

Fig. 9. IRU disturbance induced pointing error - Flight data vs. prediction via ground test [Yoshida (2012)]

3.3 Microvibration Influence on ACS

Microvibration in the high frequency region does not influence ACS in general, since the spectrum is well beyond the ACS bandwidth. However, there is an exceptional case where high frequency microvibration affects ACS, that is a gyro-induced low frequency error predicted by the authors [Takahara (2005)].

Most gyros contain analog internal loop that detects angular rate. The detected rate is then converted to the incremental angle by a V/F converter at every readout timing. Since the converter is essentially an analog integrator plus sampler with reset, aliasing occurs at this stage. Although the aliasing is suppressed by a high-order low-pass filter inserted before the converter, the filter output still has some small sensitivity to the input rate beyond the bandwidth. Consequently, if the base plate of the gyro is subject to a high frequency rotational vibration caused by any disturbance source, it is detected and is changed into a low frequency component that is below the Nyquist frequency of the sampling (see Figure 10). As a result, the ACS will receive an erroneous aliased signal from the gyro, and may respond to the signal

Figure 11 is an example of the phenomenon that was observed at the ground test of Engineering Test Satellite-8 (ETS-8,"Kiku No.8") in accordance with the prediction. The error was insignificant compared to the required attitude accuracy, since the main missions of the satellite is mobile communication experiment. But the phenomenon may be the issue for future satellites with very tight pointing requirement.

3.4 Dynamic Interface Between Mission Payload and Bus

In GOSAT(Greenhouse gases Observing Satellite) and MTSAT-2(Multi-functional Transport Satellite-2), another aspect related to disturbance-induced microvibration became an issue, that is the dynamic interface between mission payload and spacecraft bus. For satellites that carries vibration sensitive mission payload, the vibration level at the

interface plane between the payload and the S/C bus is specified. Conventionally, the acceleration level is used as the specification, that is required from the payload side based on the analysis or test with fixed-free boundary condition. But this type of specification turned out to be inadequate, since the critical frequencies of the payload is actually non-critical when the payload is onboard S/C bus. Therefore a payload-bus combined test is indispensable. Moreover, the rotation angle, in addition to the acceleration, at the I/F plane should be included to the specification [Yoshida (2011)].

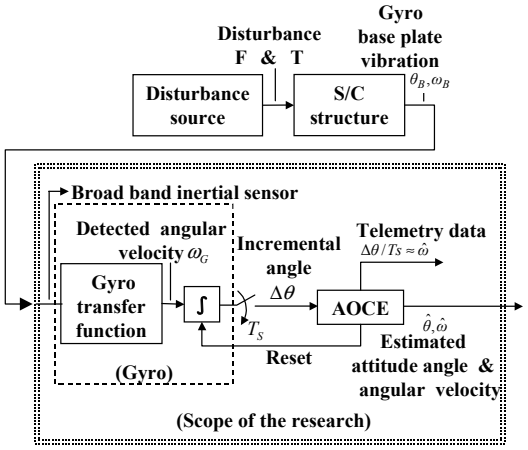

Fig. 10. Functional block diagram of AOCS [Takahara (2005)]

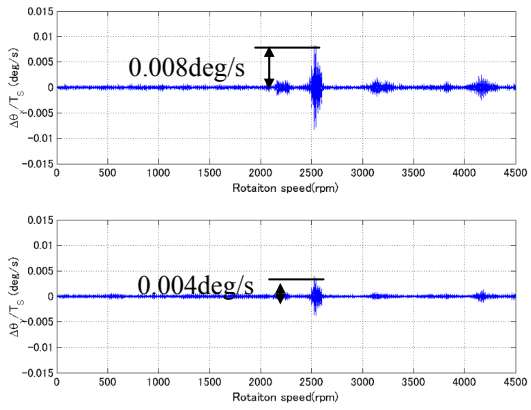

Fig. 11. Gyro output error affected by RW induced micro-vibration (ETS-8, RW4: 0-4500rpm) [Takahara (2005)]

4.CONCLUSIONS

Microvibration that is induced by many internal disturbance sources, is a central issue for spacecraft with very tight requirement of sub-micro radian class pointing stability. Technical issues are discussed, and experiences and lessons learned through the development of several satellites are presented. Specifically, the concept of low, mid and high frequency regions, and discrimination of attitude and pointing are discussed first. The new measurement methods to evaluate the pointing performance before launch are then described. Finally, microvibration influence on ACS, and the dynamic interface issue between mission payload and S/C bus are outlined.

REFERENCES

Bétermier, J. M. and Mercier, M. (1993). An Overview of CNES's Microdynamic Research Activities - Lessons Learned and On-Going Developments for Future Applications -, IAF-93-I.2.221, *44th Congress of the IAF*

Dougherty, H., et. al. (1982). Space Telescope Pointing Control System, *J. Guidance, Control & Dynamics*, Vol.5, No.4, pp.403-409

ESA (1993). *ESA Pointing Error Handbook*, ESA-NCR-502

Griffin, M. D., et. al. (1984). The Space Telescope Alternate Fine Guidance Sensor, AIAA Paper 84-1850

Kodeki, K., et. al. (2007). Development of a Correlation Tracker and a Tip-Tilt Mirror System for SOLAR-B, *J. the Japan Soc. Aeronautical & Space Sciences*, Vol. 55., No. 637, pp. 57-64 (*in Japanese*)

Jedrich, N., et. al. (2002). Cryo Cooler Induced Micro-Vibration Disturbances to Hubble Space Telescope, SPIE (NASA tech_doc N20020060462)

Kosugi, T., et. al. (2005). The Hinode (Solar-B) Mission: An Overview, *Solar Physics*, 243, Issue 1, pp.3-17

Laurens, Ph., Decoux, E. and Janvier, M. (1996). SOHO Microvibrations Analysis, Tests and Flight Results, *Proc. the 3rd Intn'l Conf. on Spacecraft Guidance, Navigation and Control Systems*, pp. 489-495

Marchante, E. M. and Muñoz, L. (1997). ARTEMIS Satellite Microvibrations Testing and Analysis Activities, *The 48th Congress of the IAF*, IAF-97-I.2.09

Schmidt, M. and Salt, D. (2012). Herschel Pointing Accuracy Improvement, *Space OPS 2012*, Stockholm, Sweden,

Takahara, O., Yoshida, N., et. al. (2004): Microvibration Transmissibility Test of SOLAR-B, *24th Intn'l Symposium on Space Science & Technology (ISTS)*, Miyazaki, Japan

Takahara, O., Yoshida, N., et. al. (2005): Study on the Method of Evaluating Microvibration Influence on Spacecraft Gyroscopes, *Proc. the 49th Space Sci. & Tech. Conf.*, 1H03, Hiroshima, Japan (*in Japanese*)

Takahara, O., Ichimoto, K., et. al. (2007). Prediction of the Pointing Stability from Ground Test and Its Initial In-orbit Evaluation of the Solar Observation Satellite SOLAR-B, *The 1st Congress of European Aerospace Society,* Berlin, Germany

Takahara, O., Yoshida, N., et. al. (2008). Study of Estimation Method of Microvibration with Simulated Satellite Structure, IAC-08-C2.3.9, *The 59th Intn'l Astronautical Congress (IAC 2008)*

Yoshida, N., Takahara, O., et. al. (2004). Systematic Approach to Achieve Fine Pointing Requirement of SOLAR-B, *16th IFAC Symposium on Automatic Control in Aerospace (ACA2004)*, St. Petersburg, Russia

Yoshida, N. (2011). Issues on Dynamic Interface between Optical Mission Payload and Spacecraft Bus, *28th ISTS*, 2011, Okinawa, Japan

Yoshida, N., Kodeki, K. and Takahara, O. (2012). Technology for Ultra-High Pointing Stability of High-Precision Observation Satellite, *Proc. the 43rd JSASS Annual Meeting*, Tokyo, Japan (*in Japanese*)

Yoshida, N. (2013). Proposed Criteria and Control Parameters for Spacecraft Transient Internal Disturbances, *29th ISTS*, June 2013, Nagoya, Japan